NJC

PAPER

View Article Online
View Journal | View Issue

Cite this: *New J. Chem.*, 2014, **38**, 1045

Aggregation-induced emission of triphenylamine substituted cyanostyrene derivatives†

Xin Zhao,[a] Pengchong Xue,[a] Kai Wang,[a] Peng Chen,[b] Peng Zhang[a] and Ran Lu*[a]

Received (in Montpellier, France) 30th October 2013,
Accepted 11th December 2013

DOI: 10.1039/c3nj01343j

www.rsc.org/njc

Cyanostyrene-based D–π–A type conjugated compounds bearing triphenylamine units (**G1**, **G1-N** and **G2**) have been synthesized. By tuning the conjugated skeleton and the electron withdrawing ability of the acceptor, green, orange and red light emitters were achieved. It is interesting that although their emissions in solutions were weak, we observed strong emission in solid states. For example, the Φ_F of the dendritic molecule **G2** in powder reached 0.67, which was more than 20 times of that in THF. The single crystal X-ray diffraction data revealed that the intermolecular H-bonds of C–H···O, C–H···N and C–H···π led to the increased rigidity of the molecular skeleton, which would restrict the intramolecular rotation, yielding high Φ_F in solid states. These AIE compounds may become candidates for emitting materials.

Introduction

Organic π-conjugated molecules have been intensively studied due to their potential applications in opto-electronic materials.[1–5] Most of the organic luminogens are highly emissive in dilute solutions but exhibit weak or quenched fluorescence upon increasing the concentrations of the solutions or in the solid states because of strong π–π interactions and the non-radiative decay process. This phenomenon, which is known as aggregation-caused quenching (ACQ),[6,7] has greatly limited the practical applications. Numerous efforts have been made to tackle this problem,[8,9] and the most important development in this field was the introduction of the term aggregation-induced emission (AIE) by Tang and co-workers in 2001.[10] They found that 1-methyl-1,2,3,4,5-pentaphenylsilole gave very weak emission in solution, but the obtained nanoparticles could emit strong fluorescence because of restriction of intramolecular rotation (RIR). Additionally, Park reported that 1-cyano-*trans*-1,2-bis-(4′-methylbiphenyl)-ethylene (CN-MBE) was non-luminescent in solution but highly emissive in the aggregated states.[11,12]

Because the achievement of the emitting materials with strong emission in solid states is important for their applications in OLEDs, laser devices, and so on, various conjugated organic molecules emitting different colors have been synthesized.[13] For example, the oligofluorenes were linked to different cores, such as porphyrin and tetraphenylsilica, to give red and blue emission in OLEDs, respectively.[14,15] The trimer of tetraphenylethene (TPE) gave a fluorescence peak at 494 nm, which shifted to 575 nm when fumaronitrile was used as a center linked to TPE units. In addition, an emission at 713 nm was achieved in the fumaronitrile-centered TPE bearing terminal *N*,*N*-diethylamino group.[16] Tian and coworkers designed a series of 2,2′-biindene-based fluorophores with strong solid-state emissions ranging from deep blue to red, which were tuned by the variation of the substituents on the 2,2′-biindenyl unit or by adjustment of the aggregation state.[17] Moreover, the luminogens emitting blue, green, and red colors constructed from tetraphenylethene, benzo-2,1,3-thiadiazole and thiophene were prepared.[18,19] It is known that triphenylamine (TPA) has been widely used as the electron donor (D) in opto-electronic materials on account of its good hole transport mobility[20–22] and the cyanostyrene is a typical electron acceptor (A) group with AIE activity.[23–25] Recently, Tian found that the multi-branched D–π–A–π–D compounds with the triphenylamine (or carbazole) group as an electron-donor and the cyanostyrene (or triazine) group as an electron-acceptor showed excellent two-photon absorption activity and AIE properties.[26]

Herein, in order to prepare new AIE materials emitting different colors we designed D–π–A conjugated compounds bearing TPA and cyanostyrene units **G1**, **G1-N** and **G2** (Scheme 1). Although their emission in solutions was weak, we observed strong emission in green, orange and red in solid states, which were tuned by the conjugation length and the electron withdrawing ability of the acceptor. For example, the second generation of triphenylamine-based dendron was

[a] *State Key Laboratory of Supramolecular Structure and Materials, College of Chemistry, Jilin University, Changchun 130012, PR China. E-mail: luran@mail.jlu.edu.cn; Fax: +86-431-88499179; Tel: +86-431-88499179*
[b] *Key Laboratory of Functional Inorganic Material Chemistry (MOE), School of Chemistry and Materials Science, Heilongjiang University, Harbin 150080, PR China*

† Electronic supplementary information (ESI) available: Electrochemical properties and ^{1}H-, ^{13}C-NMR and MALDI/TOF MS spectra. CCDC 968916 and 968917. For ESI and crystallographic data in CIF or other electronic format see DOI: 10.1039/c3nj01343j

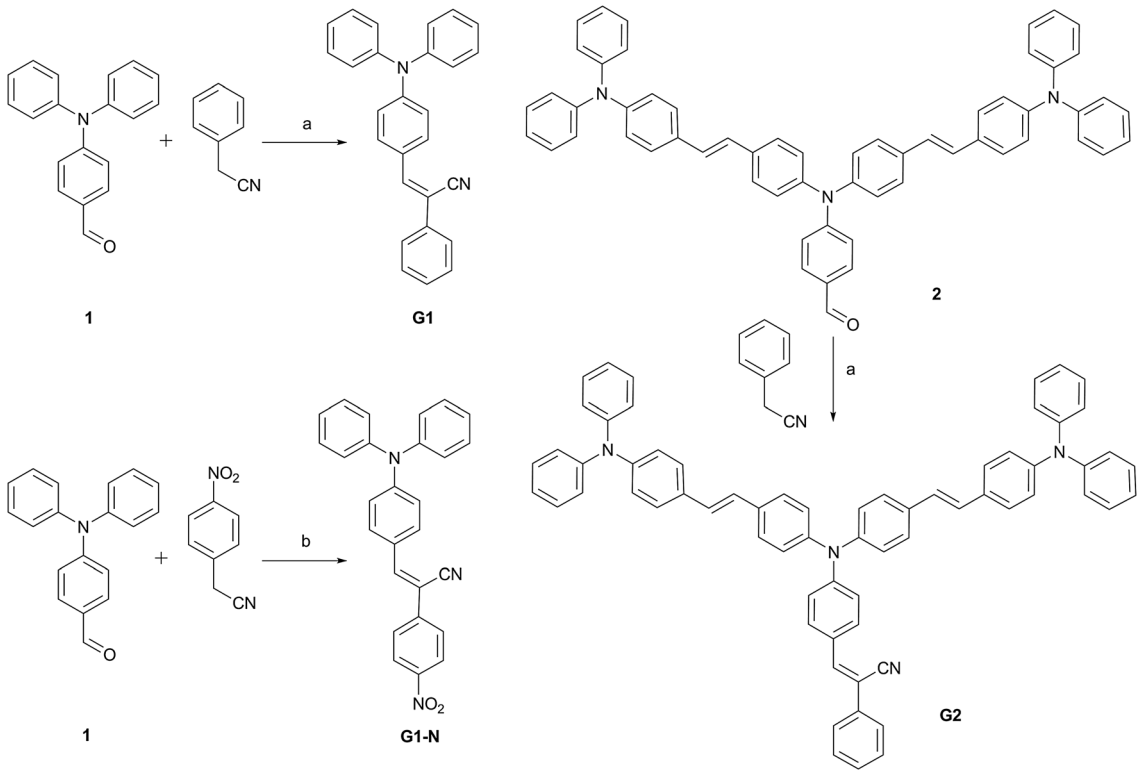

(a) NaOH, C_2H_5OH, r. t., 24h; (b) TBAH, C_2H_5OH, reflux, 12h.

Scheme 1 Synthetic routes for **G1**, **G1-N** and **G2**.

involved in **G2**[27–29] leading to larger conjugation than that of **G1**, so **G2** emitted orange light and **G1** emitted green light in solid states. When the nitro group was introduced into the cyanostyrene unit, red emitting compound **G1-N** was obtained.[30] The single crystal X-ray diffraction data revealed that the intermolecular H-bonds of C–H···O, C–H···N and C–H···π led to the increasing rigidity of the molecular skeleton, which would restrict the intramolecular rotation, yielding high Φ_F in solid states. Therefore, green, orange and red emitting compounds with AIE were obtained, which might have potential applications in organic light emitting materials.

Results and discussion

Syntheses

The synthetic routes for triphenylamine substituted cyanostyrene derivatives are described in Scheme 1. Firstly, the formyl-ended triphenylamine derivatives **1** and **2** were prepared according to the methods reported by our group previously.[31] The Knoevenagel condensation reaction between the formyl-ended triphenylamine derivative (compound **1** or **2**) and phenylacetonitrile catalyzed by sodium hydroxide afforded **G1**[32] and **G2** in a yield of 85% and 79%, respectively. Similarly, the Knoevenagel condensation reaction between compound **1** and 2-(4-nitrophenyl)acetonitrile catalyzed by tetrabutylammonium hydroxide (TBAH) gave **G1-N** in a yield of 90%. All the new compounds were characterized by FT-IR, ^{1}H NMR, ^{13}C NMR and MALDI/TOF mass spectroscopy, and they are soluble in dichloromethane, chloroform and THF. From the FT-IR spectra of **G2** we found that the vibration absorption band appeared at *ca.* 960 cm^{-1}, meaning that the carbon–carbon double bonds adopted *trans*-form. In addition, the ^{1}H NMR spectra of **G2** further confirmed that ethenyl groups adopted the *trans*-conformation on account of the absence of the signal at *ca.* 6.5 ppm assigned to the protons in *cis*-double bonds.[31]

UV-vis absorption and fluorescence emission spectra

The UV-vis absorption and fluorescence emission spectra of triphenylamine substituted cyanostyrene derivatives **G1**, **G1-N** and **G2** in THF (1.0×10^{-5} M) are shown in Fig. 1a and the corresponding photophysical data are presented in Table 1. Two clear absorption peaks at *ca.* 300 nm and 400 nm were detected for compounds **G1** and **G2**. The former one can be attributed to the π–π* transition of the triphenylamine group and the latter one can be assigned to the intramolecular charge transfer (ICT) band. In detail, the absorption bands of **G1** were located at 298 nm and 398 nm, which red-shifted to 303 nm and 406 nm for **G2** due to the enlarged conjugation of the increased dendritic structure. On account of the introduction of the nitro group the maximum absorption of **G1-N** red-shifted to 439 nm, and its absorption intensity was quite lower than that of **G1** due to the spin-forbidden charge transfer.[33] It is notable that the intensity of the absorption peaks for **G2** was higher than **G1** and **G1-N** due to the increased number of vinyl

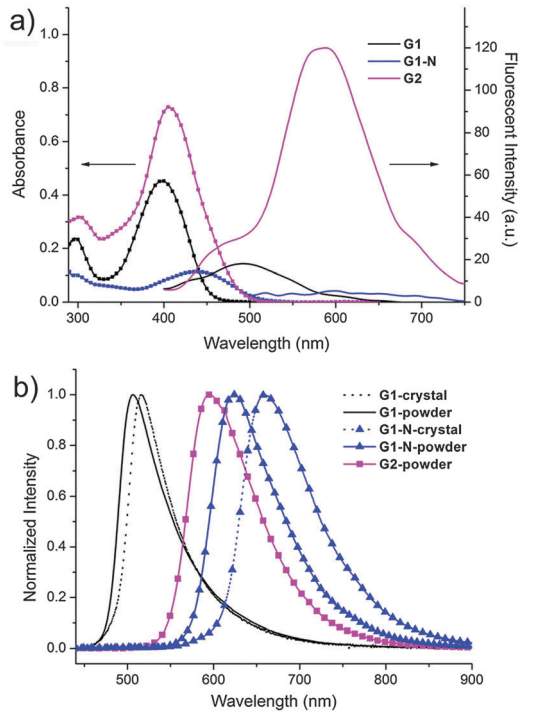

Fig. 1 (a) UV-vis absorption and fluorescence emission (λ_{ex} = 365 nm) spectra of **G1**, **G1-N** and **G2** in THF (1.0×10^{-5} M); (b) fluorescence emission spectra of **G1**, **G1-N** and **G2** in solid states (λ_{ex} = 365 nm).

Table 1 UV-vis absorption and fluorescence data for triphenylamine derivatives

	Solution		Powder		Crystal		
Molecule	λ_{abs}/nm	$\lambda_{em}{}^{a}$/nm	$\Phi_F{}^{b}$	$\lambda_{em}{}^{a}$/nm	$\Phi_F{}^{c}$	$\lambda_{em}{}^{a}$/nm	$\Phi_F{}^{c}$
G1	298, 398	494	0.02	506	0.33	516	0.31
G1-N	439	—[d]	0.01	624	0.09	658	0.06
G2	303, 406	584	0.03	596	0.67	—[d]	—[d]

[a] Excited at 365 nm. [b] Quantum yields (Φ_F) determined in THF using an integrating sphere. [c] Quantum yields (Φ_F) determined using an integrating sphere. [d] Not obtained.

triphenylamine units in **G2**. From the fluorescence emission spectra of **G1**, **G1-N** and **G2** in THF we can find that **G1-N** was almost non-emissive because the introduction of an electron withdrawing nitro group into the cyanostyrene unit might lead to the occurrence of photo-induced electron transfer from triphenylamine to the acceptor. **G1** gave a weak emission at 494 nm. Upon increasing the generation of the dendron based on triphenylamine, a red-shift of the emission band located at 584 nm was observed for **G2** due to the larger π-conjugation. The fluorescent quantum yields (Φ_F) of **G1**, **G1-N** and **G2** in THF were 0.02, 0.01 and 0.03 using an integrating sphere, meaning that the emission was very weak.

The fluorescence emission spectra of **G1**, **G1-N** and **G2** in powders or in crystals are shown in Fig. 1b. It was found that the emission of **G1** and **G2** in powders appeared at 506 nm and 596 nm, respectively, with a red-shift compared with those in solutions due to the aggregation. Although **G1-N** was non-emissive in solution, its powder gave an obvious emission at 652 nm.

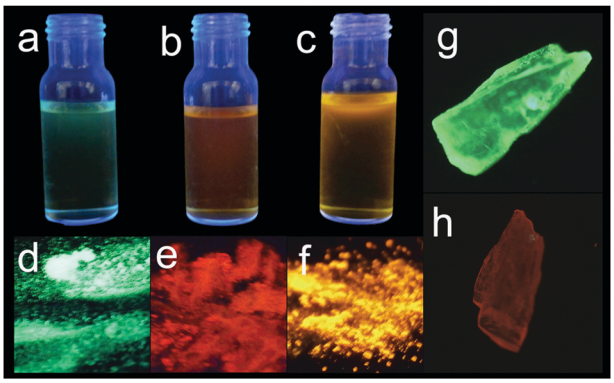

Fig. 2 Photos of **G1**, **G1-N** and **G2** in THF (a, b and c, respectively) and in powders (d, e and f, respectively) under UV illumination (365 nm), and fluorescent microscope (λ_{ex} = 330–385 nm) images of **G1** (g) and **G1-N** (h) in crystals.

Notably, the Φ_F values for these compounds in powders were more than 20 times of those in solutions (Table 1), indicating that they exhibited AIE properties. Moreover, the crystals of **G1** and **G1-N** (the crystal of **G2** was not obtained) also gave strong emission, and their emission bands further red-shifted to 516 nm and 658 nm in the crystals. The Φ_F values for **G1** and **G1-N** in crystals were 0.31 and 0.06, respectively, which were similar to those in powders. In addition, the photos of **G1**, **G1-N** and **G2** in solutions and in solid states illuminated by UV light as shown in Fig. 2 further illustrated that the emission was enhanced significantly in powders as well as in crystals compared with that in solutions.

Electrochemical properties

The electrochemical behaviors of triphenylamine substituted cyanostyrene derivatives were investigated by cyclic voltammetry (CV) using a standard three-electrode cell and an electrochemical workstation (CHI 604) under a N_2 atmosphere. Fig. 3 shows the cyclic voltammetry (CV) diagrams of **G1**, **G1-N** and **G2** using 0.1 M tetrabutylammonium tetrafluoroborate ($TBABF_4$) as a

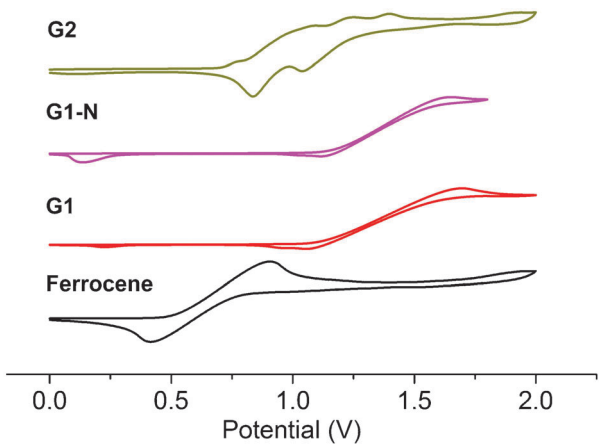

Fig. 3 Cyclic voltammograms of **G1**, **G1-N** and **G2** in CH_2Cl_2 containing 0.1 mol L^{-1} of tetrabutylammonium tetrafluoroborate ($TBABF_4$).

supporting electrolyte in dry CH_2Cl_2, glass carbon disc working electrodes, a platinum-wire counter electrode, and an SCE reference electrode. The SCE reference electrode was calibrated using the ferrocene/ferrocenium (Fc/Fc^+) redox couple as an external standard. According to the redox potential of Fc/Fc^+ (with an absolute energy level of −4.8 eV relative to the vacuum level for calibration), the HOMO energy level was calculated to be −5.52 eV for **G1**, −5.52 eV for **G1-N** and −4.91 eV for **G2** (Table S1, ESI†), respectively. The higher HOMO energy level of **G2** indicated its strong electron donating ability. The calculated LUMO energy level of **G1-N** (−3.10 eV) was lower than that of **G1** (−2.78 eV) and **G1** (−2.35 eV) due to the strong accepting ability of the nitro group.

AIE properties

As discussed above, compounds **G1**, **G1-N** and **G2** exhibited AIE behaviors. In order to evaluate the AIE properties of these compounds, **G2** was selected as an example. The UV-vis absorption and fluorescence emission spectral changes of **G2** in THF–water (**G2** is soluble in THF and water is a poor solvent) with different amounts of water are given in Fig. 4. It was found that when the amount of water was ≤50% (volume content) the UV-vis absorption spectra of **G2** were similar to that in pure THF. Upon further increasing the amount of water, the absorption band at 406 nm red-shifted and was broadened, which might be due to the molecular aggregation.[23] For example, the absorption red-shifted to 420 nm and 422 nm when the contents of water were 70% and 90% in THF–water, respectively. In addition, the appearance of tails in the visible region could be attributed to Mie scattering caused by nanoparticles.[11] From Fig. 4b, we could find that the emission of **G2** can hardly be detected when the volume content of water was ≤50% in THF–water. However, upon further increasing the amount of water in the system, the fluorescence emission of **G2** was enhanced significantly, accompanied by a blue-shift. The emission appeared at 582 nm and 573 nm when the volume contents of water were 70% and 90% in THF–water, respectively. In addition, we presented the plot of the ratio of I/I_0, in which I was the integral of fluorescence emission in the mixed solvent and I_0 was that in pure THF, *vs.* the content of water in THF–water. As shown in the inset of Fig. 4b, when the volume content of water was ≤50%, I/I_0 values were quite low. Upon increasing the content of water, I/I_0 values increased significantly, suggesting that AIE happened in the aggregates of **G2**.

X-ray studies of the single crystals

In order to reveal the mechanism of the AIE phenomena, we tried to get single crystals for all compounds. The crystals of **G1** and **G1-N** were obtained from the solutions in petroleum ether–chloroform, but we could not get the crystal of **G2**. The single crystal study revealed that the crystal structures of **G1** and **G1-N** belonged to the monoclinic space group $P2(1)/n$ and monoclinic space group $P2_1/c$, respectively, and each cell contained

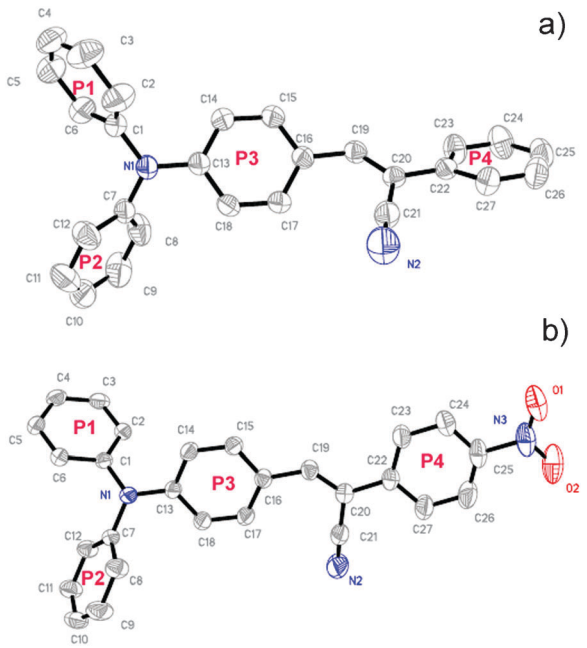

Fig. 5 ORTEP drawings of **G1** (a) and **G1-N** (b) at 50% probability level ellipsoids.

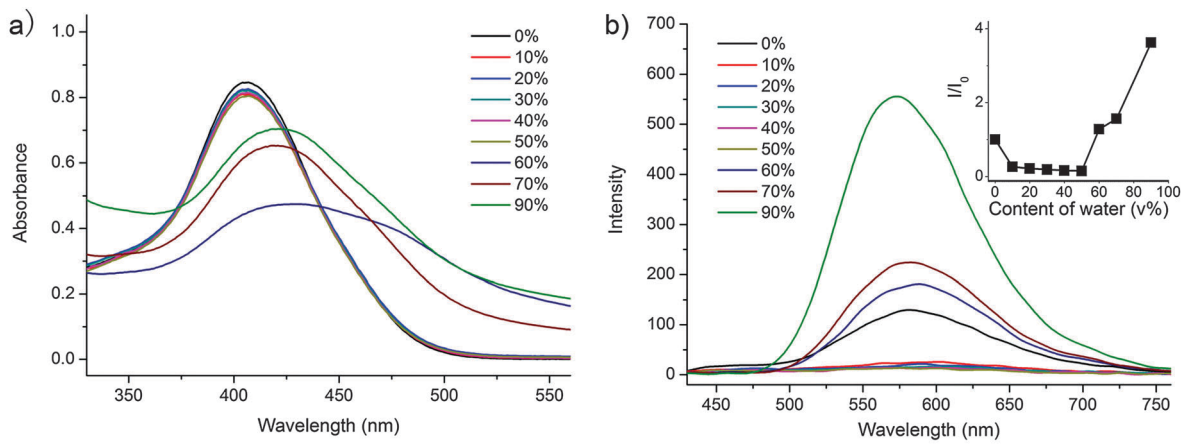

Fig. 4 (a) UV-vis absorption and (b) fluorescence emission spectra (λ_{ex} = 365 nm) of **G2** (1.0×10^{-5} M) in THF–water with different amounts of water (% volume). The inset of (b) shows a plot of PL integral *versus* water content of the solvent mixture for **G2**.

four molecules (Z = 4). The molecular ORTEP drawings are displayed in Fig. 5. In the crystal of **G1**, the torsion angle between phenyl rings P3 and P4 was 56.78(21)°, exhibiting a more twisting structure of cyanostyrene than that in **G1-N** (8.38(6)°). The twisting structures between two phenyl rings in **G1** reduce the conjugation of molecules and prevent face-to-face π–π aggregations. Moreover, the intermolecular interactions among molecules in **G1** are shown in Fig. 6a. It was found that the H-bond (2.44 Å) between N (in C–N triple bond) and the vinyl-H atom in two adjacent molecules was formed along the short axis of the molecule. The C24–H···π (P3) (2.87 Å) and C4–H···π (P3) (2.93 Å) provided two kinds of interactions for each P3 ring. These C–H···N and C–H···π interactions resulted in a rigid three-dimensional network. Thus, the twisting structure (torsion angle between P3 and P4) and the existence of multiple C–H···π H-bonds restricted the intramolecular rotation and enabled the molecule to emit light intensively in the solid states.[34] In the crystal of **G1-N** (Fig. 6b and c), the rings of P3 and P4 were almost coplanar (torsion angle 8.38(6)°) and four kinds of H-bonds were formed. C18–H···N2 (2.58 Å) and C24–H···O1 (2.62 Å) linked the molecules in each layer together along the P3 and P4 planes. Each H-bond of C2–H···O1 (2.60 Å) connected one pair of molecules in adjacent layers, and the H-bond of C5–H···O2 (2.65 Å) provided a head-to-tail type connection. Meanwhile, the C–H···π interactions of 2.61 and 2.93 Å happened between parallel non-planar molecules. Accordingly, the RIR process caused by the intermolecular interactions, including C–H···π, C–H···N and C–H···O, resulted in the increased rigidity of the molecular skeleton to yield higher Φ_F in crystals than those in solutions.

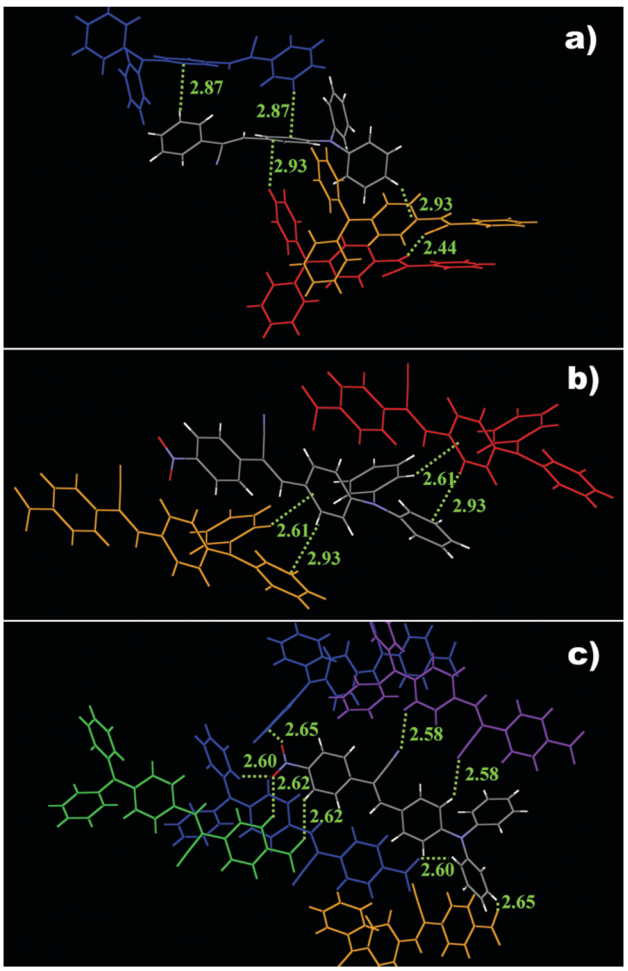

Fig. 6 Intermolecular H-bonds (C–H···O, C–H···N and C–H···π) in the crystals of **G1** (a) and **G1-N** (b, c).

Conclusions

In conclusion, cyanostyrene-based D–π–A conjugated compounds bearing triphenylamine units (**G1**, **G1-N** and **G2**) have been synthesized. By tuning the conjugated skeleton and the electron withdrawing ability of the acceptor, green, orange and red light emitters were achieved. It is interesting that although their emissions in solutions were weak, we observed strong emissions in solid states. For example, the Φ_F of dendritic molecule **G2** in powder reached 0.67, which was more than 20 times of that in THF. The single crystal X-ray diffraction data revealed that the intermolecular H-bonds of C–H···O, C–H···N and C–H···π led to the increased rigidity of the molecular skeleton, which would restrict the intramolecular rotation, yielding high Φ_F in solid states. Therefore, the green, orange and red emitting compounds with AIE properties were obtained, which might have potential applications in organic light emitting materials.

Experimental section

General

Solvents were purified and dried using standard protocols. All other chemical reagents were obtained commercially and were used as received without further purification. ^{1}H NMR spectra were recorded on a Mercury plus 400 MHz using $CDCl_3$ as solvent in all cases. ^{13}C NMR spectra were recorded on a Mercury plus 100 MHz using $CDCl_3$ as solvent. FT-IR spectra were recorded using a Germany Bruker Vertex 80v FT-IR spectrometer by incorporating samples in KBr disks. Mass spectra were recorded on an Agilent 1100 MS series and AXIMA CFR MALDI/TOF (Matrix assisted laser desorption ionization/Time-of-fight) MS (COMPACT). UV-vis absorption spectra were recorded on a Shimadzu UV-1601PC spectrophotometer. Fluorescence emission spectra were recorded on a Shimadzu RF-5301 luminescence spectrometer. The emission spectra of solids were recorded using a Maya2000 Pro CCD spectrometer. The absolute fluorescence quantum yields were measured on an Edinburgh FLS920 steady state fluorimeter. The fluorescence microscopy images were obtained using an Olympus BX51 fluorescence microscope. Cyclic voltammetry was carried out using a CHI 604B electrochemical working station at room temperature at a scan rate of 50 mV s^{-1}.

Synthetic procedures and characterization

(*Z*)-3-(4-(Diphenylamino)phenyl)-2-phenylacrylonitrile (G1). A mixture of formyl-ended triphenylamine derivative **1** (0.16 g, 0.6 mmol), phenylacetonitrile (0.11 g, 0.9 mmol), and sodium hydroxide (0.04 g, 0.9 mmol) in ethanol (50 mL) was stirred for 24 h at room temperature under an atmosphere of nitrogen. Then, the precipitate was filtered off and washed with cold ethanol. Yield: 85%. M.p. 148.0–151.0 °C. ^{1}H NMR (400 MHz, $CDCl_3$) δ 7.774 (d, J = 8 Hz, 2H), 7.642 (d, J = 8 Hz, 2H), 7.402–7.440 (m, 3H), 7.294–7.365 (m, 5H), 7.100–7.168 (m, 6H), 7.048 (d, J = 8 Hz, 2H) (Fig. S1, ESI†). ^{13}C NMR (100 MHz, $CDCl_3$) δ 149.98, 146.66, 141.73, 135.08, 130.69, 129.61, 129.02, 128.60, 126.50, 125.73, 124.41, 120.96, 118.79, 107.80 (Fig. S2, ESI†). FT-IR (KBr, cm^{-1}): 2216, 1583, 1506, 1489, 1448, 1329, 1298, 1275, 1192, 1178, 831, 760, 696. MS, *m*/*z*: cal. 372.16, found: 372.9 (Fig. S3, ESI†).

(*Z*)-3-(4-(Diphenylamino)phenyl)-2-(4-nitrophenyl)acrylonitrile (G1-N). A mixture of 4-(diphenylamino)benzaldehyde (0.16 g, 0.6 mmol), 2-(4-nitrophenyl)acetonitrile (0.15 g, 0.9 mmol), and tetrabutylammonium hydroxide (TBAH) (0.13 g, 0.9 mmol) in ethanol (50 mL) was refluxed for 12 h under an atmosphere of nitrogen. After cooling down to room temperature, the precipitate was filtered off and washed with cold ethanol to give a red solid. Yield: 90%. M.p. 160.0–162.0 °C. ^{1}H NMR (400 MHz, $CDCl_3$) δ 8.272 (d, J = 8 Hz, 2H), 7.784–7.832 (m, 4H), 7.548 (s, 1H), 7.324–7.361 (m, 4H), 7.147–7.190 (m, 6H), 7.038 (d, J = 8 Hz, 2H) (Fig. S4, ESI†). ^{13}C NMR (100 MHz, $CDCl_3$) δ 151.08, 147.24, 146.14, 144.76, 141.45, 131.50, 129.74, 126.15, 126.10, 125.13, 125.04, 124.31, 120.00, 118.11, 104.60 (Fig. S5, ESI†). FT-IR (KBr, cm^{-1}): 2218, 1574, 1514, 1485, 1340, 1284, 1198, 1180, 849, 752. MS, *m*/*z*: cal. 417.15, found: 417.2 (Fig. S6, ESI†).

(*Z*)-3-(4-(Bis(4-(4-(diphenylamino)styryl)phenyl)amino)phenyl)-2-phenylacrylonitrile (G2). **G2** was prepared from formyl-ended triphenylamine derivative **2** and phenylacetonitrile by using a similar procedure to **G1**. The crude product was purified by column chromatography (silica gel) using dichloromethane as an eluent. Yield: 85%. M.p. 112.0–116.0 °C. ^{1}H NMR (400 MHz, $CDCl_3$) δ 7.835 (d, J = 8 Hz, 2H), 7.686 (m, J = 8 Hz, 2H), 7.370–7.476 (m, 13H), 7.275–7.312 (m, 5H), 7.137–7.176 (m, 14H), 6.976–7.092 (m, 14H) (Fig. S7, ESI†). ^{13}C NMR (100 MHz, $CDCl_3$) δ 149.43, 147.57, 147.32, 145.51, 141.58, 135.03, 133.79, 131.59, 130.72, 129.31, 129.02, 128.66, 127.65, 127.45, 127.31, 127.04, 126.23, 125.76, 125.47, 124.52, 123.62, 123.06, 121.71, 118.72, 108.12, 77.37, 77.06, 76.74 (Fig. S8, ESI†). FT-IR (KBr, cm^{-1}): 2204, 1589, 1508, 1490, 1325, 1281, 1178, 960, 829, 754. MS, *m*/*z*: cal. 910.4, found: 912.4 (Fig. S9, ESI†).

X-ray crystal structure determination

Diffraction data of single crystals were collected on a Rigaku RAXIS-PRID diffractometer using the ω-scan mode with graphite-monochromator Mo·Kα radiation. The structure was solved by direct methods using the SHELXTL programs and refined by full-matrix least-squares on F^2.[35] The corresponding CCDC reference numbers are 968916 for **G1** and 968917 for **G1-N** (Table 2).

Table 2 Crystal data for **G1** and **G1-N**

Compound	G1	G2
Empirical formula	$C_{27}H_{20}N_2$	$C_{27}H_{19}N_3O_2$
Formula wt	372.45	417.45
Temperature, K	293(2) K	293(2) K
Crystal system	Monoclinic	Monoclinic
Space group	$P2(1)/n$	$P2_1/c$
a, Å	17.164(3)	11.154(2)
b, Å	6.6995(13)	7.5463(15)
c, Å	19.809(4)	25.707(5)
α/°	90.00	90.00
β/°	111.08(3)	96.42(3)
γ/°	90.00	90.00
Volume, Å^3	2125.4(7)	2150.3(7)
Z	4	4
Density, Mg m^{-3}	1.164	1.289
M (Mo Kα), mm^{-1}	0.068	0.083
Θ range, deg	3.09–27.48	3.14–27.48
No. of reflcns collected	19 408	19 989
No. of unique reflcns	4844	4896
R(int)	0.0598	0.0507
GOF	0.982	1.031
R_1 [$I > 2\sigma(I)$]	0.0535	0.0542
wR_2 [$I > 2\sigma(I)$]	0.1219	0.1212
R_1 (all data)	0.1192	0.1153
wR_2 (all data)	0.1451	0.1423

Preparation of aggregates for AIE measurements

The solution of **G2** in THF was firstly prepared (1.0×10^{-5} M). Then, 1 mL of the above solution was transferred into a volumetric flask (10 mL). After adding an appropriate amount of THF, water was added dropwise under vigorous stirring to furnish a 10 mL solution in THF–water with a specific water fraction. The water content was varied in the range of 0–90 vol%. The UV-vis absorption and fluorescence emission spectra of the resulting samples were recorded immediately after preparation.

Acknowledgements

This work was financially supported by the National Natural Science Foundation of China (51073068, 21374041), the 973 Program (2009CB939701), and the Open Project of the State Key Laboratory of Supramolecular Structure and Materials (SKLSSM201203).

Notes and references

1 P. L. Burn, S.-C. Lo and I. D. W. Samuel, *Adv. Mater.*, 2007, **19**, 1675.
2 J. Liu, Y. Cheng, Z. Xie, Y. Geng, L. Wang, X. Jing and F. Wang, *Adv. Mater.*, 2008, **20**, 1357.
3 C. Li and Z. Bo, *Polymer*, 2010, **51**, 4273.
4 H. Tian and S. Yang, *Chem. Soc. Rev.*, 2004, **33**, 85–97.
5 Y. Hong, J. W. Y. Lam and B. Z. Tang, *Chem. Soc. Rev.*, 2011, **40**, 5361.
6 R. H. Friend, R. W. Gymer, A. B. Holmes, J. H. Burroughes, R. N. Marks, C. Taliani, D. D. C. Bradley, D. A. Dos Santos, J. L. Bredas, M. Logdlund and W. R. Salaneck, *Nature*, 1999, **397**, 121.
7 S. A. Jenekhe and J. A. Osaheni, *Science*, 1994, **265**, 765.

8 S. Hecht and J. M. J. Frechet, *Angew. Chem., Int. Ed.*, 2001, **40**, 74.
9 L. Chen, S. Xu, D. McBranch and D. Whitten, *J. Am. Chem. Soc.*, 2000, **122**, 9302.
10 J. D. Luo, Z. L. Xie, J. W. Y. Lam, L. Cheng, H. Y. Chen, C. F. Qiu, H. S. Kwok, X. W. Zhan, Y. Q. Liu, D. B. Zhu and B. Z. Tang, *Chem. Commun.*, 2001, 1740.
11 B. K. An, S. K. Kwon, S. D. Jung and S. Y. Park, *J. Am. Chem. Soc.*, 2002, **124**, 14410.
12 Z. Zhao, J. W. Y. Lam and B. Z. Tang, *J. Mater. Chem.*, 2012, **22**, 23726.
13 K. E. Sapsford, L. Berti and I. L. Medintz, *Angew. Chem., Int. Ed.*, 2006, **45**, 4562.
14 B. Li, J. Li, Y. Fu and Z. Bo, *J. Am. Chem. Soc.*, 2004, **126**, 3430.
15 X. Liu, C. He, J. Huang and J. Xu, *Chem. Mater.*, 2005, **17**, 434.
16 X. Y. Shen, Y. J. Wang, E. Zhao, W. Z. Yuan, Y. Liu, P. Lu, A. Qin, Y. Ma, J. Z. Sun and B. Z. Tang, *J. Phys. Chem. C*, 2013, **117**, 7334.
17 Z. Zhang, B. Xu, J. Su, L. Shen, Y. Xie and H. Tian, *Angew. Chem., Int. Ed.*, 2011, **50**, 11654.
18 Z. Zhao, C. Deng, S. Chen, J. W. Y. Lam, W. Qin, P. Lu, Z. Wang, H. S. Kwok, Y. Ma, H. Qiu and B. Z. Tang, *Chem. Commun.*, 2011, **47**, 8847.
19 Z. Zhao, S. Chen, X. Shen, F. Mahtab, Y. Yu, P. Lu, J. W. Y. Lam, H. S. Kwok and B. Z. Tang, *Chem. Commun.*, 2010, **46**, 686.
20 Y. Tao, Q. Wang, Y. Shang, C. Yang, L. Ao, J. Qin, D. Ma and Z. Shuai, *Chem. Commun.*, 2009, 77.
21 A. Goel, M. Dixit, S. Chaurasia, A. Kumar, R. Raghunandan, P. R. Maulik and R. S. Anand, *Org. Lett.*, 2008, **10**, 2553.
22 Z. Ning and H. Tian, *Chem. Commun.*, 2009, 5483.
23 S. B. Noh, R. H. Kim, W. J. Kim, S. Kim, K.-S. Lee, N. S. Cho, H.-K. Shim, H. E. Pudavar and P. N. Prasad, *J. Mater. Chem.*, 2010, **20**, 7422.
24 Y. Li, F. Shen, H. Wang, F. He, Z. Xie, H. Zhang, Z. Wang, L. Liu, F. Li, M. Hanif, L. Ye and Y. Ma, *Chem. Mater.*, 2008, **20**, 7312.
25 S.-J. Yoon, J. W. Chung, J. Gierschner, K. S. Kim, M.-G. Choi, D. Kim and S. Y. Park, *J. Am. Chem. Soc.*, 2010, **132**, 13675.
26 W. Huang, F. Tang, B. Li, J. Su and H. Tian, *J. Mater. Chem. C*, 2014, DOI: 10.1039/c3tc31913j.
27 T. H. Xu, R. Lu, X. P. Qiu, X. L. Liu, P. C. Xue, C. H. Tan, C. Y. Bao and Y. Y. Zhao, *Eur. J. Org. Chem.*, 2006, 4014.
28 T. Xu, R. Lu, X. Liu, P. Chen, X. Qiu and Y. Zhao, *J. Org. Chem.*, 2008, **73**, 1809.
29 X. Qiu, R. Lu, H. Zhou, X. Zhang, T. Xu, X. Liu and Y. Zhao, *Tetrahedron Lett.*, 2007, **48**, 7582.
30 J. A. Marsden, J. J. Miller, L. D. Shirtcliff and M. M. Haley, *J. Am. Chem. Soc.*, 2005, **127**, 2464.
31 J. Jia, K. Cao, P. Xue, Y. Zhang, H. Zhou and R. Lu, *Tetrahedron*, 2012, **68**, 3626.
32 B. Li, Q. Li, B. Liu, Y. Yue and M. Yu, *Dyes Pigm.*, 2011, **88**, 301.
33 H. Kotaka, G.-i. Konishi and K. Mizuno, *Tetrahedron Lett.*, 2010, **51**, 181.
34 X. Y. Shen, W. Z. Yuan, Y. Liu, Q. Zhao, P. Lu, Y. Ma, I. D. Williams, A. Qin, J. Z. Sun and B. Z. Tang, *J. Phys. Chem. C*, 2012, **116**, 10541.
35 SHELXTL, Version 5.1; Siemens Industrial Automation, Inc. 1997; G. M. Sheldrick, SHELXS-97, Program for Crystal Structure Solution; University of Göttingen, Göttingen, 1997.